JOURNAL OF Bioactive and Compatible Polymers

Article

Journal of Bioactive and Compatible Polymers
26(1) 20–34
© The Author(s) 2011
Reprints and permissions:
sagepub.co.uk/journalsPermissions.nav
DOI: 10.1177/0883911510392007
jbc.sagepub.com
SAGE

Poly(vinyl alcohol)-based electrospun meshes as potential candidate scaffolds in regenerative medicine

Dario Puppi[1], Anna Maria Piras[1], Nicola Detta[1], Hanna Ylikauppila[2], Lila Nikkola[2], Nureddin Ashammakhi[2], Federica Chiellini[1] and Emo Chiellini[1]

Abstract

Fibrous meshes based on three different poly(vinyl alcohol) (PVA) polymers, with 12% vinyl acetate monomeric units and molar weights of 37,000, 67,000, and 130,000 were developed as potential scaffolds for regenerative medical applications. The meshes were electrospun and characterized by molecular weight, concentration, applied voltage, and needle–collector distance. The influence of feed rate and the electrodes configuration (needle-to-tip and screen-to-screen system) was determined. Highly porous, 3D structures composed of randomly oriented ultrafine fibers, with an average fiber diameter of a few hundred nanometers were developed. Solutions of PVA and human serum albumin were successfully electrospun and the fibrous mesh was stabilized with glutaraldehyde. The influence of these operations on the mechanical properties was evaluated by uniaxial tensile testing.

Keywords

biomaterials, electrospinning, nanofibers, poly(vinylalcohol), polymer processing

Introduction

Regenerative medical research involves creating products that replace or regenerate human cells, tissues, or organs in order to restore or establish normal function.[1] The common

[1]Laboratory of Bioactive Polymeric Materials for Biomedical and Environmental Applications (BIOlab), Department of Chemistry and Industrial Chemistry, University of Pisa, via Vecchia Livornese 1291, 56010 San Piero a Grado (Pi), Italy
[2]Department of Biomedical Engineering, Tampere University of Technology, PO Box 589 (Hermiankatu 12 B), FIN-33101 Tampere, Finland

Corresponding author:
Emo Chiellini, Laboratory of Bioactive Polymeric Materials for Biomedical and Environmental Applications (BIOlab), Department of Chemistry and Industrial Chemistry, University of Pisa, via Vecchia Livornese 1291, 56010 San Piero a Grado (Pi), Italy
Email: emochie@dcci.unipi.it

Downloaded from jbc.sagepub.com at PENNSYLVANIA STATE UNIV on September 17, 2016

tissue engineering goal is the development of constructs that can meet individual tissue defects by means of biodegradable matrices (scaffolds) that provide cells with a temporary structure that mimics the functions of the native extra cellular matrix (ECM), serve as an adhesion substrate for cells, provide mechanical support, and guide the growing tissue.[2]

To accomplish these objectives, scaffold materials must be carefully selected and the architecture properly designed. The topographic reaction of cells, nanometer range features, and nanoscale material structuring has been investigated to control cell behavior. Three-dimensional (3D) scaffolds using electrospun nanofibers have been developed to produce nonwoven nanofiber assemblies that mimic the nanosized structure of ECM of natural tissues.[2–4] Highly porous structure and high spatial interconnectivity of electrospun matrix that resemble a natural ECM are necessary for cells to maintain their phenotypic shape and establish natural behavior patterns.[5]

The possibility of processing various materials (either biodegradable or biostable) and exploiting different loading methodologies (electrospinning of drug solutions or suspensions, coaxial spinning, multi-syringe feeding) make electrospinning a versatile technique for the production of nanofibers loaded with a broad variety of active agents, including proteins,[6,7] anti-inflammatory agents,[8–11] antibiotics,[12–14] anticancer drugs,[15–17] DNA,[18] and growth factors.[19] The high surface area of nanofibers along with the high and interconnected porosity of electrospun meshes enhance mass transfer phenomena involved in drug release.[4,20]

Poly(vinyl alcohol) (PVA) is a hydrophilic polymer with good thermal and chemical stabilities; it is manufactured on an industrial scale by polymerizing vinyl acetate (VAc) followed by hydrolysis.[21] Different degrees of hydrolysis effect water solubility, chemical properties,[21–25] and crystallinity.[26,27] Because of its good mechanical properties, biocompatibility, and nontoxicity,[28] PVA has been proposed for various biomedical applications, such as drug delivery systems, wound dressing, artificial skin, and cardiovascular devices.

Electrospinning of PVA and the parameters affecting fiber morphology, such as polymer concentration and electric field,[29,30] polymer molecular weight (Mw),[31,32] surface tension,[33] and pH[34] have been investigated, as well as the addition of inorganic fillers,[35–38] drugs,[30,39,40] and enzymes.[41] Changes in the hydrolysis of PVA have shown to influence solution properties,[30] such as surface tension and conductivity, as well as the morphology and mechanical properties of the resulting electrospun meshes.[30,42] However, very little has been published with respect to PVA hydrolysis $\leq$96% and on electrospinning of PVA with a low degree of hydrolysis, with deference to processing conditions on fiber morphology.

The aim of this study was to optimize the electrospinning parameters for the production of fibrous meshes of PVA with 88% hydrolysis as potential scaffolds for regenerative medicine. Therefore, the relationship between fiber morphology and processing conditions was investigated with respect to polymer Mw and concentration, electric field parameters, solution feed rate, and cross-linking. In addition, the conditions for the production of PVA nanofibers loaded with human serum albumin (HSA), as model of water-soluble bioactive agents, were investigated. The influence on the mechanical properties of both HSA loading and cross-linking was examined.

Downloaded from jbc.sagepub.com at PENNSYLVANIA STATE UNIV on September 17, 2016

Materials and methods

Materials

The 88% hydrolized PVAs were supplied by Erkol S.A. (Spain) and used as delivered as follows; PVA 05/88 is (88%, PVA 37,000 Mw), PVA 08/88 (88% PVA, 67,000 Mw), and PVA18/88 (88% PVA,130,000 Mw), respectively. HSA powder (96–99%) was purchased from Sigma (Italy) and used as received. Type III laboratory-grade pure water was obtained from ELIX/RiOs Pretreatment Pack (Millipore, Italy) equipped with PROGARD 02™ with vent filter (Millipore, Italy).

Preparation of electrospun meshes

PVA solutions with concentrations in the range 5–20% w/v were prepared by dissolving the polymer in deionized water, with gentle stirring for 4 h at 40°C. For the protein-loaded meshes, the HSA ($Conc_{HSA}$) was dissolved in PVA solution at room temperature, and the mixture stirred until complete dissolution (~1 h).

To fabricate polymer meshes, the PVA solutions were loaded into a syringe fitted with a metallic needle (0.84 mm ID). An electric field was created between the tip of the needle and an electrically grounded aluminum screen by applying a high voltage to the needle, using a bipolar Electrostatic Generator Chargemaster BP50 (SIMCO, The Netherlands) or a SL300 power supply (Spellman High Voltage, UK). To determine the optimal electrical field parameters for electrospinning jet stability, various combinations between applied voltage (V) and needle tip to collector distance (d) were investigated varying V in the range of 20–60 kV and d from 10 to 40 cm. The solution feed rate was either driven by gravity or controlled by a syringe pump (BSP99-N, Braintree Scientific, MA) (Figure 2(a) and (b)). In the latter case, it was varied between 1 and 5 mL/h.

The influence of a screen-to-screen (Sc–Sc) electrode configuration on fiber morphology was evaluated by employing an apparatus with two parallel metallic screens at different electrical potentials. One functioned as an auxiliary electrode and the other one as a fiber collector (Figure 3(a)). The solution was fed at a given flow rate to the metallic needle jutting out of an aperture in the middle of one plate and the fibers were collected onto the other plate.

The electrospinning process was performed at room temperature and humidity under a fume hood with controlled aeration. The processing time was 5 min for a preliminary morphology investigation and 2 h for the production of meshes for detailed characterization. All the electrospun meshes were dried under vacuum for 24 h and left in a dessicator. Electrospinning conditions for the production of fibrous meshes are reported in Table 1.

Glutaraldehyde cross-linking

Some electrospun samples were cross-linked with glutaraldehyde (GA) following the procedure by Wang et al.[43] Briefly, electrospun samples were immersed in 10 mL of acetone solution containing 28 μL of GA (30 mM) and 8 μL of HCl (0.01 N). After 24 h, the samples were washed with acetone several times and placed in a vacuum chamber for 24 h. To determine mesh stability and water uptake, three cross-linked slab samples ($15 \times 15\,mm^2$, 600–700 μm thick) with a dry weight of ~30 mg were immersed in water; at

Downloaded from jbc.sagepub.com at PENNSYLVANIA STATE UNIV on September 17, 2016

specific time intervals, dabbed dry, and weighed. The swelling degree (SD%) at each time point was calculated as:

$$SD = ((W_{sw} - W_d)/W_d) \times 100 \quad (1)$$

where W_{sw} was the weight after incubation in water and W_d the initial weight.

Morphological analysis

Electrospun samples were cut, gold sputtered, and observed by scanning electron microscopy (SEM, model JEOL JSM 300, Japan). The top surface of the produced meshes was analyzed and the average diameter of electrospun fibers was determined by means of Image J 1.36b software on SEM micrographs with a $1000\times$ magnification. The fiber diameter was calculated over 30 measurements per specimen, taken from randomly selected fields.

Mechanical characterization

Uniaxial tensile properties of meshes were evaluated at room temperature with an Instron 5564 (Instron, MA) by following the standard ASTM D 1708-93, EN ISO 9073-2, and ASTM D 882-91 protocols.[44–47] Six dog bone shaped samples, ($38 \times 15\,mm^2$ overall in size, $5 \times 22\,mm^2$ in the gage area) were cut out from visibly defect-free parts of the electrospun disk and the average thickness was calculated from micrometer (Vogel Srl, Italy) measurements in the load-bearing part of each sample. The specimens were stretched to the break point at room temperature and ambient humidity, under a constant crosshead displacement of 10 mm/min. Tensile stress–strain curves, elastic modulus, stress, and strain at break were obtained from a software recording data (Merlin); mesh yield strength was determined by the offset method, considering as offset a strain of 0.2%.

Statistical evaluation

Quantitative data were presented as mean ± standard deviation (SD). Data sets consisting of average fiber diameter or mechanical properties were screened by one-way ANOVA and a Tukey test was used for *post hoc* analysis; significance was defined at $p < 0.05$.

Results and discussion

In this study, the optimization of electrospinning PVA (88% hydrolysis) for the production of 3D nanofiber meshes, as potential scaffolds for tissue regeneration applications, was investigated. The influence of processing parameters on the mesh morphology was evaluated to determine the suitability of these meshes for tissue engineering scaffolds. Cross-linking the electrospun PVA, to enhance stability in aqueous environments, was explored as well as the influence of HSA loading and chemical cross-linking on mesh mechanical properties.

Investigation of electrospinning parameters

The influence of electrospinning parameters on the morphology of PVA meshes (SEM analysis) was evaluated by varying the polymer Mw and concentration, employing different electric field parameters (V and d), adding HSA to the polymer solution, employing two different types of

Downloaded from jbc.sagepub.com at PENNSYLVANIA STATE UNIV on September 17, 2016

control over solution feed and two different electrode–counterelectrode configurations. Statistical analysis was performed to evaluate significant differences in average fiber diameter.

Effect of polymer Mw and concentration

After a preliminary investigation, two V–d combinations (40 kV–15 cm and 60 kV–25 cm) were used that provided a stable electrospinning jet. Applying these electrical fields and employing a solution feed rate that was controlled by gravity, polymer concentration ranges, as function of polymer Mw, were investigated to produce uniform fibers; the optimal ranges were 15–20% w/v for PVA5/88, 10–20% w/v for PVA8/88, and 5–7.5% w/v for PVA18/88. Processing lower concentrations produced beaded structures or beads-on-string structures that are typical when electrospinning low concentrations; while at very high concentrations, the droplet dried out at the tip of the needle outlet, thus compromising the process.

The SEM analysis of the meshes in selected concentration ranges revealed highly porous, 3D structure mats composed of randomly oriented fibers (Figure 1(a)–(i)). The average fiber diameter ranged between 100 and 400 nm, depending on processing conditions (Table 1). Some defects in the form of bead and fiber bonding, typical of low-viscosity solutions were observed in meshes obtained from 15% w/v polymer solutions (Figure 1(a)). By increasing the polymer concentration to 20% w/v, a more uniform fiber morphology was obtained (Figure 1(b)). The micrographs of the PVA8/88 meshes (Figure 1(d) and (e)) were similar to the PVA5/88 meshes and the formation of beads along the fibers was inhibited by increasing the polymer concentration.

A comparison of the data obtained from the dimensional analysis of PVA8/88 and PVA5/88 fibers (Table 1), using the same processing parameters, showed that an increase in the Mw caused a significant increase in fiber diameter ($p < 0.01$). In addition, the increase of PVA8/88 concentration in the range 10–20% w/v resulted in an average diameter increase ($p < 0.01$). The PVA18/88 meshes, produced using 5% w/v solutions, were nonuniform fibrous structures (Figure 1(g)). Increasing the polymer concentration to 7.5% w/v, improved the mesh morphology, although some bead-on-string structure was still observable (Figure 1(h)).

The polymer concentration affected solution viscosity and surface tension, which are the key parameters in the electrospinning process. These should be within a range to allow effective polymer chain entanglement, which is necessary to obtain a stable electrospinning jet and restrain the effects of surface tension. If sufficient chain entanglement is not achieved, the solution jet breaks up into droplets while traveling toward the collector. However, too high concentrations can compromise the process because of the cohesive nature of high viscosity solutions and because of the difficulty of controlling the solution feed rate to the needle tip.[4,12,13,48] For a given concentration, polymers with higher Mw can provide a higher degree of chain entanglement.[49] Our findings, in agreement with the current literature, demonstrated a relationship between polymer Mw and minimum polymer concentration to produce uniform fibers as well as the fiber dimensions.[15,31,48–54]

Effect of electric field parameters

As previously discussed, we found two V/d combinations (40 kV–15 cm and 60 kV–25 cm) that provide a stable electrospinning jet and, consequently, for the production of uniform

Downloaded from jbc.sagepub.com at PENNSYLVANIA STATE UNIV on September 17, 2016

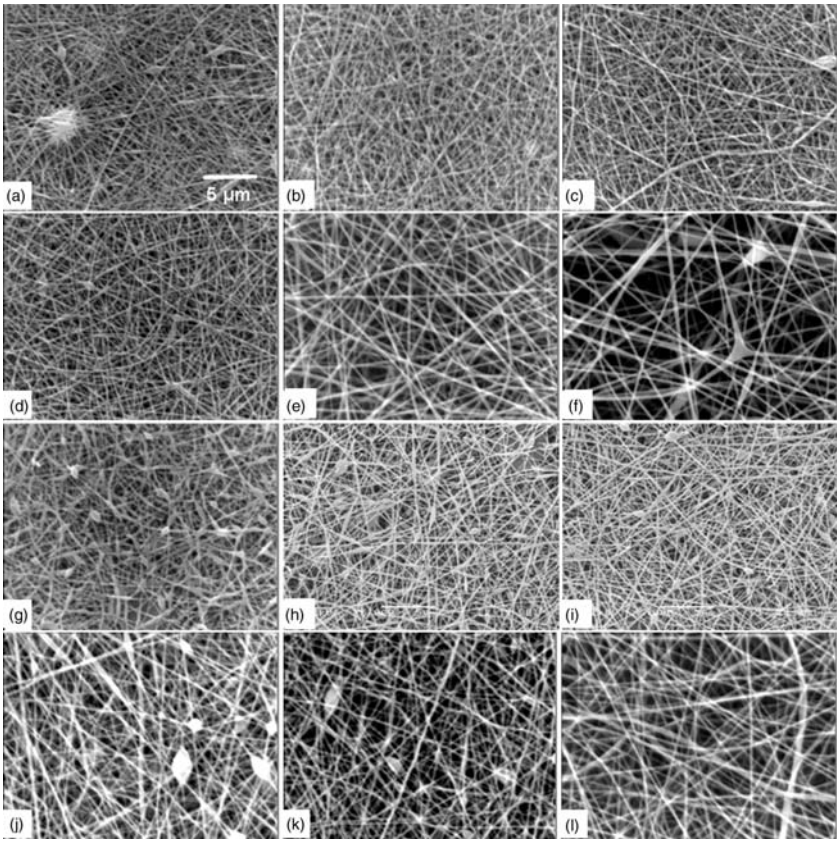

Figure 1. SEM images of PVA meshes. PVA 5/88 meshes: (a) $C = 15\%$, $V = 40$ kV, $d = 15$ cm; (b) $C = 20\%$, $V = 40$ kV, $d = 15$ cm; and (c) $C = 20\%$, $V = 60$ kV, $d = 25$ cm. PVA 8/88 meshes: (d) $C = 10\%$, $V = 40$ kV, $d = 15$ cm; (e) $C = 15\%$, $V = 40$ kV, $d = 15$ cm; and (f) $C = 15\%$, $V = 60$ KV, $d = 25$ cm. PVA 18/88 meshes: (g) $C = 5\%$, $V = 40$ kV, $d = 15$ cm; (h) $C = 7.5\%$, $V = 40$ kV, $d = 15$ cm; and (i) $C = 7.5\%$, $V = 60$ kV, $d = 25$ cm. PVA/HSA meshes: (j) $Conc_{HSA} = 0.5\%$, $V = 40$ kV, $d = 15$ cm; (k) $Conc_{HSA} = 2\%$, $V = 40$ kV, $d = 15$ cm; and (l) $Conc_{HSA} = 2\%$, $V = 60$ kV, $d = 25$ cm.
Note: Magnification 5000×, scale bar on micrograph 1a is applicable to all micrographs

fibrous structures. A comparison of the micrographs of mesh samples produced by applying two different V/d combinations (40 kV–15 cm and 60 kV–25 cm) while keeping all other parameters constant, showed that the morphology of the meshes from both PVA5/88 and PVA18/88 were not significantly affected by the changes in the electric field parameters (Figure 1(c) and (d)). In contrast, these changes affected the distance between fibers in the PVA8/88 mesh and consequently the fiber packing density (Figure 1(f)). The average fiber diameter in meshes from 10% w/v PVA8/88 solution was the only statistically significant difference ($p < 0.01$) that was seen due to the changes made in the voltage–distance combination.

For a given distance between electrodes, with other variables constant, there was a minimum critical applied voltage needed to obtain a stable electrospun jet with a uniform fibrous structure. Below this value, the electrostatic repulsion forces between the electrodes

Downloaded from jbc.sagepub.com at PENNSYLVANIA STATE UNIV on September 17, 2016

Table 1. Average fiber diameter of PVA meshes produced employing various processing conditions

Polymer	PVA Concentration % (w/v)	HSA Concentration % (w/v)	*V* kV	*d* cm	Fiber diameter	
					Average (nm)	SD (nm)
PVA5/88	15		40	15	126	36
PVA5/88	15		60	25	150	53
PVA5/88	20		40	15	140	40
PVA5/88	20		60	25	160	63
PVA8/88	10		40	15	159	26
PVA8/88	10		60	25	246	49
PVA8/88	15		40	15	249	51
PVA8/88	15		60	25	274	78
PVA8/88	20		40	15	350	59
PVA8/88	20		60	25	395	91
PVA18/88	5		40	15	238	88
PVA18/88	5		60	25	–	–
PVA18/88	7.5		40	15	136	46
PVA18/88	7.5		60	25	141	48
PVA8/88	15	0.5	40	15	279	66
PVA8/88	15	0.5	60	25	235	46
PVA8/88	15	1	40	15	246	64
PVA8/88	15	1	60	25	241	65
PVA8/88	15	2	40	15	257	66
PVA8/88	15	2	60	25	240	73

did not provide a drawing stress value strong enough to prevent bead formation.[4,55,56] An increase in the applied voltage produced a less stable jet that would split and splay, which eventually led to a broader distribution of fiber diameters.[48,57] As reported, variations in needle–collector distance have an effect on polymer fiber shape and diameter.[30,57–59] In general, a specific distance is required to allow the fibers sufficient time to dry before reaching the collector.[3]

In our research, the electric field strength values (2.67 kV/cm for 45 kV–15 cm and 2.4 kV/cm for 60 kV–25 cm) were comparable with one another. This may be the reason why no marked differences in mesh morphology were observed. After examining the effects of polymer concentration and Mw, and the electric field parameters, we decided to characterize electrospun meshes made from PVA8/88, using 15% w/v concentration, $V = 40$ kV and $d = 15$ cm, which gave the best results in terms of mesh morphology and fiber dimension.

Effect of HSA

To produce composite PVA/HSA fibers, solutions of PVA8/88 (15% w/v) and HSA (0.5–2% w/v) were electrospun applying $V = 40$ kV and $d = 15$ cm. The addition of HSA to the polymer solution did not affect the resulting electrospun meshes as nonwoven fibrous structures (Figure 1(j) and (k)). Statistical analysis showed that there was not any significant difference between the average fiber diameters of plain and HSA-loaded meshes that were electrospun under the same conditions (Table 1). The loaded meshes did seem to

Downloaded from jbc.sagepub.com at PENNSYLVANIA STATE UNIV on September 17, 2016

have a lower fiber packing density and some beads along the fibers were observed. As suggested by Zhang et al.,[30] the increased solution conductivity due to the addition of HSA, together with the possible formation of PVA–protein secondary bonding, can compromise the stability of the electrospinning jet inducing the formation of beads.

Effect of feed rate

The rate of the solution feed to the needle tip was driven by gravity, employing an L-shaped syringe. Therefore, the feed rate conditions, such as the effect of the variation of the fluid level into the syringe, were controlled by frequent addition of solution to the syringe. The feed rate was estimated to range between 2 and 10 mL/h depending on the processing conditions employed.

The reproducibility of the feed rate by means of a syringe pump was investigated using 15% w/v solution of PVA8/88, applying $V = 40$ kV and $d = 15$ cm. Three different flow rates (1, 3, and 5 mL/h) were investigated. The SEM micrographs (Figure 2(a) and (b) vs. Figure 1(e)) and fiber dimension data (Tables 1 and 2) of the electrospun meshes produced using the syringe pump, exhibit similar morphology but significantly lower average fiber diameter ($p < 0.01$) than those produced by gravity feed. The differences in the average fiber diameters obtained employing the three different feed rates were not statistically significant. Moreover, an increase in the feed rate inhibited the formation of beads and spindles.

Variations in feed rate also influence the jet velocity and the material transfer rate which can affect fiber morphology and diameter. By increasing the feeding rate, more solution is ejected from the tip of the needle in a given time; therefore, if the electric force is able to stretch the jet sufficiently, the resulting fibers will have larger diameters, otherwise beads are formed because of surface tension.[4,12,13,30,55] However, the influence of solution feed rate is less at lower polymer concentrations.[49] Although, the inhibition of fiber defect formation by decreasing feed rate is known,[12,13,30] we observed spindle formation in the fibers electrospun at lower feed rates; this formation was inhibited by increasing the feed rate. These findings are in agreement with Du et al.,[60] even though the reason for the formation of defects at low feed rate is not clear.

Effect of screen-to-screen (Sc–Sc) configuration

To obtain a more uniform electric field, a Sc–Sc configuration was assembled by setting two parallel metal plates as electrodes (Figure 3(a)). As reported in other papers,[15,50] this

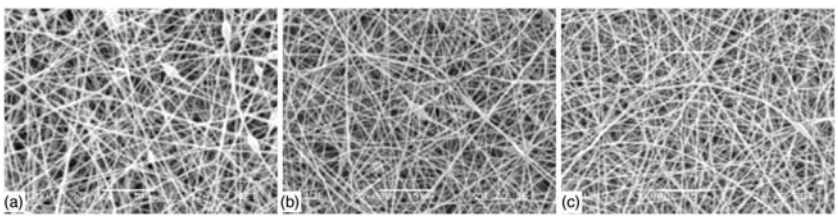

Figure 2. SEM micrographs of 15% PVA8/88 meshes ($V = 40$ kV, $d = 15$ cm) collected with controlled feeding rate (magnification 5000×): (a) $F = 1$ mL/h; (b) $F = 3$ mL/h; and (c) $F = 5$ mL/h

Downloaded from jbc.sagepub.com at PENNSYLVANIA STATE UNIV on September 17, 2016

configuration was used for the development of 3D electrospun meshes based on other polymeric materials. The conditions for the electrospinning of 15% w/v water solutions of PVA8/88 were $V = 40$ kV, $d = 15$ cm and a distance between the two screens (d_1) of 18 cm. Employing this Sc–Sc configuration, we obtained focused fiber collections by minimizing the area where the fibers are deposited (Figure 3(b)). Compared to the meshes produced employing the conventional needle to screen (NtS) configuration, thicker meshes with smaller round shapes were obtained. This allowed for the production of electrospun disks with uniform thicknesses (larger than 1 mm) in a shorter processing time depending on the solution feed rate. A PVA8/88 mesh 1.4 mm thick and 8 cm diameter was produced in about 2 h (Figure 3(c)).

In comparison to the meshes fabricated with the NtS configuration, we observed a similar mesh morphology (Figure 3(d)) that was not significantly different in average fiber diameter (Table 2) but with the overall advantage of inhibiting the formation of beads at the three feed rates (1, 3, and 5 mL/h). Moreover, like in the NtS configuration, there were no significant differences among average fiber diameters obtained by employing different feed rates.

The Sc–Sc configuration allows electric fields with nearly parallel lines by applying different voltages to the two screens,[61] which are different to those achieved in the conventional NtS configuration where a potential difference is applied between a needle tip and a large collector. A more uniform electric field allowed us to reduce fiber collection area, thus obtaining meshes with larger and more uniform thickness. The optimized conditions that we employed for the production of PVA8/88 meshes in studies

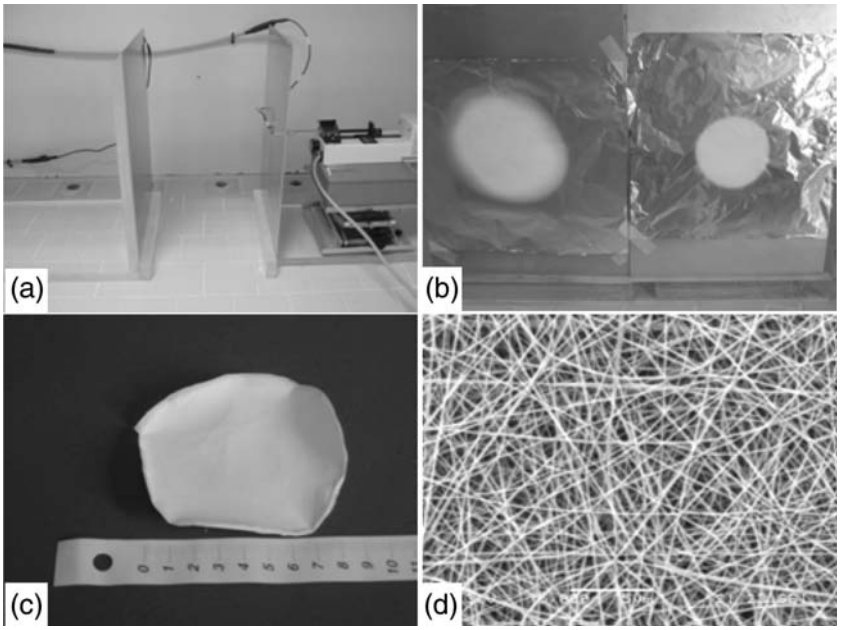

Figure 3. (a) Sc–Sc configuration; (b) PVA8/88 fiber depositions obtained by means of NtS (left) and Sc–Sc configuration (right); (c) PVA8/88 electrospun disk (thickness ≅ 1.4 mm, diameter ≅ 8 cm) produced under Sc–Sc configuration; and (d) SEM micrograph (magnification 5000×) of PVA8/88 mesh produced under Sc–Sc configuration ($F = 5$ mL/h)

Downloaded from jbc.sagepub.com at PENNSYLVANIA STATE UNIV on September 17, 2016

Table 2. Fiber diameter of PVA8/88 meshes produced using a syringe pump and either a NtS or a Sc–Sc electrode configuration

F (mL/h)	Electrodes configuration	Fiber diameter	
		Average (nm)	SD (nm)
1	NtS	161	25
1	Sc–Sc	158	37
3	NtS	164	31
3	Sc–Sc	172	45
5	NtS	175	34
5	Sc–Sc	166	39

$C = 15\%$ w/v; $V = 40$ kV; $d = 15$ cm; $d_1 = 18$ cm.

regarding GA cross-linking and mechanical testing were $V = 40\,\text{kV}$, $d = 15\,\text{cm}$, $d_1 = 18\,\text{cm}$, and $F = 5\,\text{mL/h}$.

GA cross-linking

The stability of the fibrous structure of electrospun PVA meshes was compromised after immersion in an aqueous environment because of the polymer hydrophilicity. However, the structure of fully hydrolyzed PVA meshes can be preserved in water by physical or chemical cross-linking of the polymer chains.[30,33,38,43,62] GA cross-linking of electrospun PVA with 96–99% hydrolysis was applied to partially hydrolyzed PVA8/88 meshes.[42,43] The cross-linked samples were immersed in water and weighed at prefixed time intervals to determine the swelling degree. After cross-linking, the mesh morphology was investigated by SEM following immersion in water (Figure 4).

Cross-linking did not alter the mesh morphology and the fibrous structure was maintained for 4 days in water. The cross-linked meshes reached a ~500% swelling which practically remained constant during 4 days of soaking. However, some morphology defects, probably due to partial polymer dissolution, were observed immediately after soaking in water.

Currently, concerns regarding the cytotoxicity of unreacted GA are limiting its bioapplications. Therefore, in this study, the electrospun samples were washed several times in acetone to remove the residual GA after cross-linking. However, studies assessing the cytocompatibility of the cross-linked PVA and the effect of possible release of GA need to be undertaken in detail.

Mechanical characterization

Tensile mechanical properties of plain PVA meshes, PVA/HSA meshes ($\text{Conc}_{\text{HSA}} = 2\%$ w/v) and cross-linked PVA meshes were compared by tensile testing. Representative stress–strain curves of PVA meshes are exhibited in Figure 5(a). Both the HSA loading and GA cross-linking caused a significant decrease in the elastic modulus, stress at break and elongation at break (Figure 5(b)–(d)). In comparison to plain PVA meshes, the yield strength was comparable in the case of PVA/HSA meshes but higher in the case of cross-linked meshes (Figure 5(e)).

Downloaded from jbc.sagepub.com at PENNSYLVANIA STATE UNIV on September 17, 2016

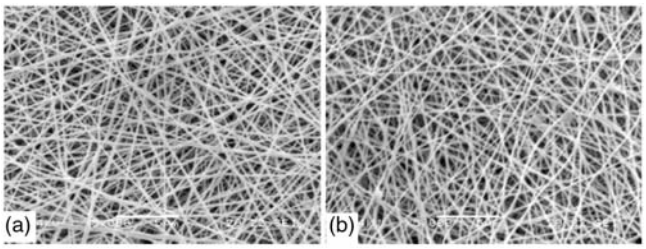

Figure 4. SEM micrographs of cross-linked PVA8/88 meshes (magnification 5000×): (a) before immersion and (b) after immersion in water

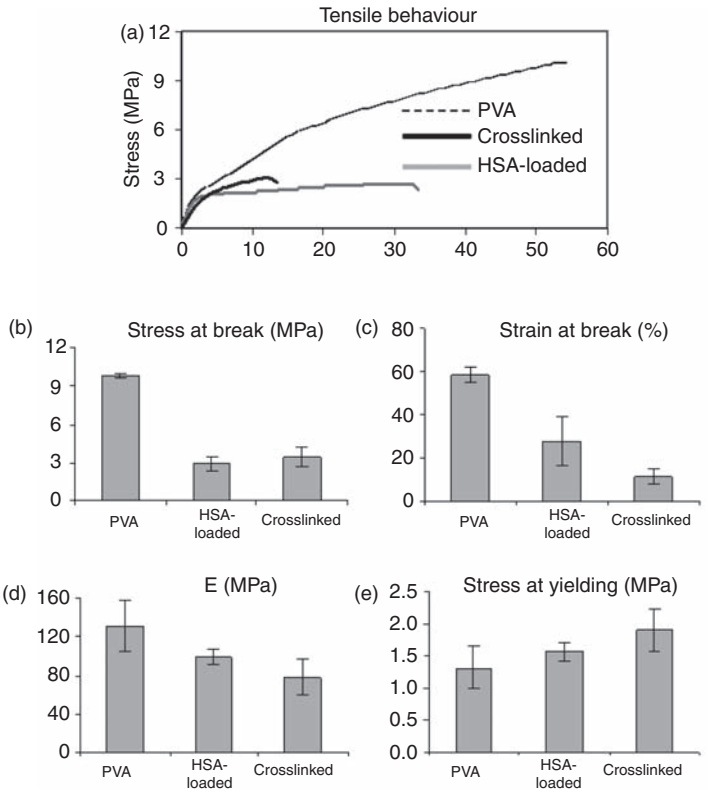

Figure 5. Tensile mechanical properties of PVA8/88 meshes: (a) representative stress–strain curves; (b) peak stress; (c) strain at break; (d) elastic modulus; and (e) yielding strength

The effect of HSA loading on mechanical strength of electrospun meshes seems to be consistent with what reported by Chew et al.[63] in the assessment of the tensile behavior of single electrospun poly(caprolactone-*co*-ethylene methyl phosphate) fibers loaded with bovine serum albumin. They found that protein encapsulation resulted in weaker and more brittle fibers indicating that the effect could be due to a phase separation between the protein and polymer, resulting in the restriction of polymer chain movement and elongation at the interface of these two regions.

Downloaded from jbc.sagepub.com at PENNSYLVANIA STATE UNIV on September 17, 2016

GA acts as chemical cross-linker by forming inter- and intra-chain acetyl bridges by covalent bonding with hydroxyl groups of PVA.[28,64–67] Previous work on electrospun meshes of 98% hydrolyzed PVA showed that after GA cross-linking, the strength at break increased while the elongation at break decreased.[43] In this study, the yield strength of PVA meshes was increased by cross-linking, but the ultimate strength was decreased after cross-linking. The introduction of cross-linking agent, besides causing the formation of a chemical cross-linked network that tends to reduce chain mobility and flexibility,[68] also affects the crystallinity and the physical network due to hydrogen bonding between polymer chains.[69] The mechanical behavior of fibrous meshes is influenced by factors other than single fiber mechanical properties, such as fiber packing density and fiber–fiber bonding interaction,[70] which can be affected by the chemical cross-linking process. Although the tensile strength of a single fiber is increased by cross-linking, in our experience, additional factors, other than fiber mechanics, are prominent in controlling mesh mechanical response.

Conclusions

The conditions for electrospinning PVA (88% hydrolysis degree) with three different Mws were optimized. 3D collections of PVA fiber with diameter in the range of hundreds of nanometers were fabricated using different polymer concentrations depending on polymer Mw. It was possible to control fiber diameter size by changing polymer Mw and concentration. PVA8/88 meshes were further characterized for the optimization of processing conditions, HSA loading, chemical cross-linking, and tensile mechanical properties.

Changing the solution feed rate to needle tip had no significant influence on PVA8/88 fibers dimension but affected bead formation. The Sc–Sc configuration provided a more focused fiber collection and the production of PVA8/88 electrospun disks 1.4 mm thick. GA cross-linking of electrospun PVA8/88 did not change mesh morphology; cross-linked mats improved stability in aqueous environment with a swelling degree of ~500% in water for 4 days. Uniaxial tensile tests showed that both HSA loading and GA cross-linking diminished stress and strain at break but GA cross-linking increased yielding strength.

The conditions for the electrospinning of PVA solutions were optimized to allow easy loading of water-soluble bioactive agents into 3D nanofiber meshes. The developed meshes can be easily loaded with proteins by simply adding the loading agent to the water solution avoiding the use of harsh organic solvents that could compromise its bioactivity, and can be stabilized in water by means of chemical cross-linking. HSA was used as model protein susceptible to incorporate hydrophobic agents and to host positive interaction with different cell cultures.

These meshes are currently being tested for their cytocompatibility with regard to GA residue, drug loading efficiency, and release kinetics. This research will serve as a base for growth factors releasing scaffolds for tissue engineering applications.

Acknowledgements

This study was done within the framework of the European Network of Excellence 'EXPERTISSUES' (Project NMP3-CT-2004-500283) with the partial financial support provided by INSTM Prisma Project, PRIN – 2006 – prot. 2006038548. Authors thank Mr Piero Narducci of Univesity of Pisa in recording SEM images.

Downloaded from jbc.sagepub.com at PENNSYLVANIA STATE UNIV on September 17, 2016

References

1. Mason C and Dunnill P. A brief definition of regenerative medicine. *Reg Med* 2007; 3: 1–5.
2. Puppi D, Chiellini F, Piras AM and Chiellini E. Polymeric materials for bone and cartilage repair. *Prog Polym Sci* 2010; 35: 403–440.
3. Pham QP, Sharma U and Mikos AG. Electrospinning of polymeric nanofibers for tissue engineering applications: a review. *Tissue Eng* 2006; 12: 1197–1211.
4. Detta N, Puppi D, Errico C, Chiellini F, Piras AM and Chiellini E. Polymeric nanofiber constructs in drug delivery and tissue engineering. In: Chaughule RS and Ramanujan R (eds) *Nanoparticles: synthesis, characterization and applications*. Stevenson Ranch, CA: American Scientific Publishers, 2010, pp.271–291.
5. Stevens MM and George JH. Exploring and engineering the cell surface interface. *Science* 2005; 310: 1135–1138.
6. Kim TG, Lee DS and Park TG. Controlled protein release from electrospun biodegradable fiber mesh composed of poly(ε-caprolactone) and poly(ethylene oxide). *Int J Pharm* 2007; 338: 276–283.
7. Maretschek S, Greiner A and Kissel T. Electrospun biodegradable nanofiber nonwovens for controlled release of proteins. *J Control Release* 2008; 127: 180–187.
8. Nikkola L, Seppälä J, Harlin A, Ndreu A and Ashammakhi N. Electrospun multifunctional diclofenac sodium releasing nanoscaffold. *J Nanosci Nanotechnol* 2006; 6: 3290–3295.
9. Piras AM, Nikkola L, Chiellini F, Ashammakhi N and Chiellini E. Development of diclofenac sodium releasing bio-erodible polymeric nanomats. *J Nanosci Nanotechnol* 2006; 6: 3310–3320.
10. Jiang H, Fang D, Hsiao B, Chu B and Chen W. Preparation and characterization of ibuprofen-loaded poly(lactide-co-glycolide)/poly(ethylene glycol)-g-chitosan electrospun membranes. *J Biomater Sci Polym Ed* 2004; 15: 279–296.
11. Piras AM, Chiellini F, Chiellini E, Nikkola L and Ashammakhi N. New multicomponent bioerodible electrospun nanofibers for dual-controlled drug release. *J Bioact Compatible Polym* 2008; 23: 423–443.
12. Zong X, Kim K, Fang D, Ran S, Hsiao BS and Chu B. Structure and process relationship of electrospun bioabsorbable nanofiber membranes. *Polymer* 2002; 43: 4403–4412.
13. Zong XH, Li S, Chen E, Garlick B, Kim K-S, Fang D, et al. Prevention of Postsurgery-induced abdominal adhesions by electrospun bioabsorbable nanofibrous poly(lactide-co-glycolide)-based membranes. *Ann Surg* 2004; 240: 910–915.
14. Volpato FZ, Ramos SLF, Motta A and Migliaresi C. Physical and in-vitro biological evaluation of a PA6/MWCNT electrospun composite for biomedical applications. *J Bioactive Compat Polym* 2011; 26: 35–47.
15. Puppi D, Piras AM, Detta N, Dinucci D and Chiellini F. Poly(lactic-co-glycolic acid) electrospun fibrous meshes for the controlled release of retinoic acid. *Acta Biomater* 2010; 6: 1258–1268.
16. Xie J and Wang C-H. Electrospun micro- and nanofibers for sustained delivery of paclitaxel to treat C6 Glioma in vitro. *Pharm Res* 2006; 23: 1817–1826.
17. Puppi, D., Piras, A.M., Chiellini, F., Chiellini, E., Martins, A., Leonor, I.B. et al. Optimized electro- and wet-spinning techniques for the production of polymeric fibrous scaffolds loaded with bisphosphonate and hydroxyapatite, *J Tissue Eng Regen Med* 2010, doi: 10.1002/term.310.
18. Luu YK, Kim K, Hsiao BS, Chu B and Hadjiargyrou M. Development of a nanostructured DNA delivery scaffold via electrospinning of PLGA and PLA-PEG block copolymers. *J Control Release* 2003; 89: 341–353.
19. Chew SY, Wen J, Yim EKF and Leong KW. Sustained release of proteins from electrospun biodegradable fibers. *Biomacromolecules* 2005; 6: 2017–2024.
20. Sill TJ and von Recum HA. Electrospinning: applications in drug delivery and tissue engineering. *Biomaterials* 2008; 29: 1989–2006.
21. Chiellini E, Corti A, D'Antone S and Solaro R. Biodegradation of poly(vinyl alcohol) based materials. *Prog Polym Sci* 2003; 28: 963–1014.
22. Pereira APV, Vasconcelos WL and Oréfice RL. Novel multicomponent silicate-poly(vinyl alcohol) hybrids with controlled reactivity. *J Non-Cryst Solids* 2000; 273: 180–185.
23. Tang Y-F, Du Y-M, Hu X-W, Shi X-W and Kennedy JF. Rheological characterisation of a novel thermosensitive chitosan/poly(vinyl alcohol) blend hydrogel. *Carbohydr Polym* 2007; 67: 491–499.
24. Mansur HS, Sadahira CM, Souza AN and Mansur AAP. FTIR spectroscopy characterization of poly (vinyl alcohol) hydrogel with different hydrolysis degree and chemically

Downloaded from jbc.sagepub.com at PENNSYLVANIA STATE UNIV on September 17, 2016

crosslinked with glutaraldehyde. *Mater Sci Eng C* 2008; 28: 539–548.

25. Finch CA. (ed.) *Polyvinyl alcohol, properties and applications*. New York: Wiley, 1973.
26. Hassan C and Peppas N. Structure and applications of poly(vinyl alcohol) hydrogels produced by conventional crosslinking or by freezing/thawing methods. In: Dušek K (ed.) *Biopolymers PVA hydrogels, anionic polymerisation nanocomposites*. Berlin, Heidelberg: Springer-Verlag, 2000, pp.37–65.
27. Finch CA. Appendix 2 health and toxicity regulations relating to polyvinyl alcohol. In: Finch CA (ed.) *Polyvinyl alcohol developments*. Aylesbury, UK: John Wiley & Sons, 1992, pp.763–765.
28. Yamaoka T, Tabata Y and Ikada Y. Comparison of body distribution of poly(vinyl alcohol) with other water-soluble polymers after intravenous administration. *J Pharm Pharmacol* 1995; 47: 479–486.
29. Bin D, Hak-Yong K, Se-Chul L, Chang-Lu S, Douk-Rae L, Soo-Jin P, et al. Preparation and characterization of a nanoscale poly(vinyl alcohol) fiber aggregate produced by an electrospinning method. *J Polym Sci Part B: Polym Phys* 2002; 40: 1261–1268.
30. Zhang C, Yuan X, Wu L, Han Y and Sheng J. Study on morphology of electrospun poly(vinyl alcohol) mats. *Eur Polym J* 2005; 41: 423–432.
31. Koski A, Yim K and Shivkumar S. Effect of molecular weight on fibrous PVA produced by electrospinning. *Mater Lett* 2004; 58: 493–497.
32. Jun Z, Hou H, Wendorff JH and Greiner A. Poly(vinyl alcohol) nanofibres by electrospinning: influence of molecular weight on fibre shape. *e-Polymers* 2005; 38: 1–7.
33. Yao L, Haas TW, Guiseppi-Elie A, Bowlin GL, Simpson DG and Wnek GE. Electrospinning and stabilization of fully hydrolyzed poly(vinyl alcohol) fibers. *Chem Mater* 2003; 15: 1860–1864.
34. Son WK, Youk JH, Lee TS and Park WH. Effect of pH on electrospinning of poly(vinyl alcohol). *Mater Lett* 2005; 59: 1571–1575.
35. Shao C, Kim H-Y, Gong J, Ding B, Lee D-R and Park S-J. Fiber mats of poly(vinyl alcohol)/silica composite via electrospinning. *Mater Lett* 2003; 57: 1579–1584.
36. Gong J, Li X-D, Ding B, Lee D-R and Kim H-Y. Preparation and characterization of H4SiMo12O40/poly(vinyl alcohol) fiber mats produced by an electrospinning method. *J Appl Polym Sci* 2003; 89: 1573–1578.
37. Siddheswaran R, Sankar R, Babu MR, Rathnakumari M, Jayavel R, Murugakoothan P, et al. Preparation and characterization of ZnO nanofibers by electrospinning. *Cryst Res Technol* 2006; 41: 446–449.
38. Hong KH, Park JL, Sul IH, Youk JH and Kang TJ. Preparation of antimicrobial poly(vinyl alcohol) nanofibers containing silver nanoparticles. *J Polym Sci Part B: Polym Phys* 2006; 44: 2468–2474.
39. Zeng J, Aigner A, Czubayko F, Kissel T, Wendorff JH and Greiner A. Poly(vinyl alcohol) nanofibers by electrospinning as a protein delivery system and the retardation of enzyme release by additional polymer coatings. *Biomacromolecules* 2005; 6: 1484–1488.
40. Spasova M, Manolova N, Naydenov M, Kuzmanova J and Rashkov I. Electrospun biohybrid materials for plant biocontrol containing chitosan and *Trichoderma Viride* spores. *J Bioactive Compat Polym* 2011; 26: 48–55.
41. Stoilova O, Manolova N, Gabrovska K, Marinov I, Godjevargova T, Mita DG and Rashkov I. Electrospun polyacrylonitrile nanofibrous membranes tailored for acetylcholinesterase immobilization. *Compatible Polym* 2010; 25: 40–57.
42. Wang X, Fang D, Yoon K, Hsiao BS and Chu B. High performance ultrafiltration composite membranes based on poly(vinyl alcohol) hydrogel coating on crosslinked nanofibrous poly(vinyl alcohol) scaffold. *J Membr Sci* 2006; 278: 261–268.
43. Wang X, Chen X, Yoon K, Fang D, Hsiao BS and Chu B. High flux filtration medium based on nanofibrous substrate with hydrophilic nanocomposite coating. *Environ Sci Technol* 2005; 39: 7684–7691.
44. ASTM. *Standard test method for tensile properties of plastics by use of microtensile specimens, ASTM D1708*. West Conshohocken, PA: ASTM, 1993.
45. ASTM. *Standard test methods for tensile properties of thin plastic sheeting, ASTM D 882*. West Conshohocken, PA: ASTM, 1991.
46. ISO. *Textiles. Test methods for nonwovens. Part 2: Determination of thickness, EN ISO 9073-2*. Geneva: Switzerland: ISO, 1995.
47. Maniglio D, Bonani W, Bortoluzzi G, Servoli E, Motta A and Migliaresi C. Electrodeposition of silk fibroin on metal substrates. *J Bioactive Compat Polym* 2010; 25: 441–454.
48. Deitzel JM, Kleinmeyer J, Harris D and Beck Tan NC. The effect of processing variables on the morphology of electrospun nanofibers and textiles. *Polymer* 2001; 42: 261–272.

Downloaded from jbc.sagepub.com at PENNSYLVANIA STATE UNIV on September 17, 2016

49. Tan SH, Inai R, Kotaki M and Ramakrishna S. Systematic parameter study for ultra-fine fiber fabrication via electrospinning process. *Polymer* 2005; 46: 6128–6134.
50. Puppi, D., Detta, N., Piras, A.M., Chiellini, F., Clarke, D.A., Reilly, G.C. et al. Development of electrospun three-arm star poly(ε-caprolactone) meshes for tissue engineering application, *Macromol Biosci* 2010; 10: 887–897.
51. Gupta P, Elkins C, Long TE and Wilkes GL. Electrospinning of linear homopolymers of poly(methyl methacrylate): exploring relationships between fiber formation, viscosity, molecular weight and concentration in a good solvent. *Polymer* 2005; 46: 4799–4810.
52. Geng X, Kwon O-H and Jang J. Electrospinning of chitosan dissolved in concentrated acetic acid solution. *Biomaterials* 2005; 26: 5427–5432.
53. Demir MM, Yilgor I, Yilgor E and Erman B. Electrospinning of polyurethane fibers. *Polymer* 2002; 43: 3303–3309.
54. Ki CS, Baek DH, Gang KD, Lee KH, Um IC and Park YH. Characterization of gelatin nanofiber prepared from gelatin-formic acid solution. *Polymer* 2005; 46: 5094–5102.
55. Zuo W, Zhu M, Yang W, Yu H, Chen Y and Zhang Y. Experimental study on relationship between jet instability and formation of beaded fibers during electrospinning. *Polym Eng Sci* 2005; 45: 704–709.
56. Lee KH, Kim HY, Bang HJ, Jung YH and Lee SG. The change of bead morphology formed on electrospun polystyrene fibers. *Polymer* 2003; 44: 4029–4034.
57. Moroni L, Licht R, de Boer J, de Wijn JR and van Blitterswijk CA. Fiber diameter and texture of electrospun PEOT/PBT scaffolds influence human mesenchymal stem cell proliferation and morphology, and the release of incorporated compounds. *Biomaterials* 2006; 27: 4911–4922.
58. Megelski S, Stephens JS, Chase DB and Rabolt JF. Micro- and nanostructured surface morphology on electrospun polymer fibers. *Macromolecules* 2002; 35: 8456–8466.
59. Lee JS, Choi KH, Ghim HD, Kim SS, Chun DH, Kim HY, et al. Role of molecular weight of atactic poly(vinyl alcohol) (PVA) in the structure and properties of PVA nanofabric prepared by electrospinning. *J Appl Polym Sci* 2004; 93: 1638–1646.
60. Du J, Shintay S and Zhang X. Diameter control of electrospun polyacrylonitrile/iron acetylacetonate ultrafine nanofibers. *J Polym Sci Part B: Polym Phys* 2008; 46: 1611–1618.
61. Shin YM, Hohman MM, Brenner MP and Rutledge GC. Experimental characterization of electrospinning: the electrically forced jet and instabilities. *Polymer,* 2001; 42: 09955–09967.
62. Ding B, Kim H-Y, Lee S-C, Shao C-L, Lee D-R, Park S-J, et al. Preparation and characterization of a nanoscale poly(vinyl alcohol) fiber aggregate produced by an electrospinning method. *J Polym Sci Part B: Polym Phys* 2002; 40: 1261–1268.
63. Chew SY, Hufnagel TC, Lim CT and Leong KW. Mechanical properties of single electrospun drug-encapsulated nanofibres. *Nanotechnology* 2006; 17: 3880–3891.
64. Yeom C-K and Lee K-H. Pervaporation separation of water-acetic acid mixtures through poly(vinyl alcohol) membranes crosslinked with glutaraldehyde. *J Membr Sci* 1996; 109: 257–265.
65. Rhim JW, Yeom C-K and Kim S-W. Modification of poly(vinyl alcohol) membranes using sulfur-succinic acid and its application to pervaporation separation of water-alcohol mixtures. *J Appl Polym Sci* 1998; 68: 1717–1723.
66. Durmaz-Hilmioglu N, Yildirim AE, Sakaoglu AS and Tulbentci S. Acetic acid dehydration by pervaporation. *Chem Eng Process* 2001; 40: 263–267.
67. Yu J, Lee CH and Hong WH. Performances of crosslinked asymmetric poly(vinyl alcohol) membranes for isopropanol dehydration by pervaporation. *Chem Eng Process* 2002; 41: 693–698.
68. Andrade G, Barbosa-Stancioli E, Mansur A, Vasconcelos W and Mansur H. Small-angle X-ray scattering and FTIR characterization of nanostructured poly(vinyl alcohol)/silicate hybrids for immunoassay applications. *J Mater Sci* 2008; 43: 450–463.
69. Krumova M, López D, Benavente R, Mijangos C and Pereña JM. Effect of crosslinking on the mechanical and thermal properties of poly(vinyl alcohol). *Polymer* 2000; 41: 9265–9272.
70. Zhang H and Chen Z. Fabrication and characterization of electrospun PLGA/MWNTs/hydroxyapatite biocomposite scaffolds for bone tissue engineering. *J Bioactive Compat Polym* 2010; 25: 241–259.

Downloaded from jbc.sagepub.com at PENNSYLVANIA STATE UNIV on September 17, 2016